Quantum dots: lasers and amplifiers

2003 J. Phys.: Condens. Matter 15 R1063

(http://iopscience.iop.org/0953-8984/15/24/201)

INSTITUTE OF PHYSICS PUBLISHING JOURNAL OF PHYSICS: CONDENSED MATTER

J. Phys.: Condens. Matter **15** (2003) R1063–R1076 PII: S0953-8984(03)34901-X

TOPICAL REVIEW

Quantum dots: lasers and amplifiers

Dieter Bimberg and Nikolai Ledentsov[1]

Institut für Festkörperphysik, PN5-2, Technische Universität Berlin, Hardenbergstraße 36, 10623, Germany

Received 20 February 2003
Published 6 June 2003
Online at stacks.iop.org/JPhysCM/15/R1063

Abstract

Continuous wave room-temperature output power of ∼3 W for edge emitters and of 1.2 mW for vertical-cavity surface-emitting lasers is realized for GaAs-based devices using InAs quantum dots (QDs) operating at 1.3 μm. Characteristic temperatures up to 170 K below 330 K are realized. Simultaneously, differential efficiency exceeds 80% for these devices. Lasers emitting up to 12 W at 1140–1160 nm are useful as pump sources for Tm^{3+}-doped fibres for frequency up-conversion to 470 nm. Both types of lasers show transparency current densities of 6 A cm^{-2} per dot layer, $\eta_{int} = 98\%$ and α_i around 1.5 cm^{-1}. Long operation lifetimes (above 3000 h at 50 °C heatsink temperature at 1.5 W CW) and improved radiation hardness as compared to quantum well (QW) devices are manifested. Cut-off frequencies of about 10 GHz at 1100 nm and 6 GHz at 1300 nm and low α factors resulting in reduced filamentation and improved M^2 values in single-mode operation are realized. Quantum dot semiconductor optical amplifiers (QD SOAs) demonstrate gain recovery times of 120–140 fs, 4–7 times faster than bulk/QW SOAs. The breakthrough became possible due to the development of self-organized growth in QD technology.

Contents

1. Introduction 1064
2. Growth 1065
3. Edge-emitting lasers 1066
   3.1. Basic characteristics 1066
   3.2. Temperature stability 1067
   3.3. Single-mode operation and filamentation problem 1067
   3.4. Mode grouping 1069
   3.5. Operational lifetime and accelerated degradation tests 1071
   3.6. Time response 1071
4. Vertical cavity surface-emitting lasers 1072

[1] On leave from: Abraham F Ioffe Physical Technical Institute, Politekhnicheskaya 26, 194021, St Petersburg, Russia.

0953-8984/03/241063+14$30.00

5. QD amplifiers 1075
6. Conclusion 1075
Acknowledgments 1075
References 1076

1. Introduction

Recently, remarkable progress in the understanding of the universal phenomena of self-organization of epitaxial nanostructures on crystal surfaces of semiconductors has been achieved [1, 2]. This progress resulted in the formation of quantum dots (QDs), with such excellent properties that many different fields of device applications emerged [3–6]. The electronic and optical properties of self-organized QDs correspond to those of single atoms [7], rather than solids.

QD lasers represent an ultimate case of the application of the size quantization concept to semiconductor heterostructure lasers [8], an approach which previously resulted in the successful development of QW devices. In their patent, Dingle and Henry [8] proposed that size quantization effects, resulting in a strong modification of the density of states, are very advantageous when used for the active media of semiconductor lasers, as they allow suppression of the states at high energies. These states are responsible for the degradation of device performance at high temperatures, as the carriers effectively populate high energy states with temperature increase, reducing the population of the near-bandedge states responsible for lasing. Moreover, in size-quantized heterostructures the density of states at the bandedge is also strongly increased. Size quantization in more than one direction causes a singularity in the density of states near the bandedge [8], as was stressed by Dingle and Henry.

However, in spite of the fact that more than two decades have passed since it was predicted that quantum wire and QD lasers should be more superior to classical lasers [1, 8–10], the progress in this field remained slow until the early 1990s.

Amongst the anticipated advantages of QD lasers were [9, 10]:

- decreased transparency current,
- increased material gain,
- large characteristic temperature T_0 (which characterizes the stability of the threshold current with temperature increase),
- increased differential gain,
- decreased α factor and chirp (shift of the lasing wavelength with current).

The original predictions were generally based on simplified assumptions [9] of:

- infinite barriers,
- ideal QDs of identical shape,
- temperature-insensitive homogeneous broadening,
- one confined electron and hole level,
- bimolecular e–h recombination,
- ultrafast energy relaxation of injected carriers,
- equilibrium carrier distribution,
- lattice matched heterostructures and similar confinement volume for electrons and holes.

In realistic devices these assumptions had to be replaced in recent years by different ones:

- finite barriers,
- size and shape dispersion of QDs,

- many electron and hole levels and the impact of the continuum states,
- monomolecular (excitonic) recombination,
- non-equilibrium carrier distribution,
- strained heterostructures with completely different potential wells for electrons and holes,

leading now to more realistic theoretical predictions [1, 11–16] for lasers. For example, temperature stability of the threshold current can be either lower or higher, depending on the particular size, shape, number of electron and hole levels and density of the QDs.

The first such QD lasers were created by us in 1993 and early 1994 [17]. The overwhelming potential advantages of QDs have been verified today on actual devices [1, 11–17] and new previously unexpected advantages were demonstrated. It appeared, for example, that the use of QDs in diode lasers also has several decisive technological advantages:

(i) Largely extended wavelength control by QD size and composition on a given substrate. Lasing wavelengths at 1.3XX μm spectral range is realized, and lasing in 1.4XX and 1.5XX μm spectral ranges important for telecom and free-space applications can also be potentially achieved using GaAs substrates.

(ii) Very low threshold current densities (<7 A cm^{-2} per QD sheet) and, simultaneously, very low internal losses ($\sim$1–3 cm^{-1}) and high quantum efficiencies ($>$80–96%) are demonstrated.

(iii) Carrier confinement in narrow gap QDs placed in a wide gap matrix can prevent nonequilibrium carrier spreading and nonradiative recombination. This improves radiation hardness [18] and suppresses the facet overheating, increasing the catastrophic optical mirror damage (COMD) level [19].

(iv) In many cases, the advantages of QDs are still not even well understood. Quite surprisingly semiconductor optical amplifiers (SOAs) based on QD GaAs show remarkable promise to outperform InGaAsP bulk and QW SOAs, as in the case of lasers since QD SOAs show gain recovery times of 140 fs, 4–7 times faster than classical ones [20, 21]. Additional advantages of QD SOAs are reduced chirp [11], larger saturated gain [22], no cross-gain modulation [23], etc.

2. Growth

The technique of QD fabrication that was later applied for current-injection GaAs-based QD lasers employs the self-organized growth of uniform nanometre-scale islands [1–5]. It is known that a layer of a material having a lattice constant different from that of the substrate, after some critical thickness is deposited, may spontaneously transform to an array of three-dimensional islands. It was demonstrated for the example of InGaAs QDs on a GaAs surface that there exists a range of deposition parameters, where the islands are small ($\sim$10 nm), have a similar size and shape and form dense arrays [1–5]. Due to the strain-induced renormalization of the surface energy of the facets, an array of equisized and equishaped 3D islands may represent a stable state of the system [24], as manifested by the process reversibility studies upon temperature ramping experiments [25]. In contrast, deviation from the optimal range of growth conditions results in ultrafast ripening of the islands within only a few seconds. Interaction of the equilibrium islands via the substrate also allows their lateral ordering [1, 2, 4, 5]. From a different point of view the existence of the equilibrium size does not necessarily mean that this size is always to be reached; smaller islands can be used as well. At the same time, the existence of the equilibrium size is extremely important in practice, as it allows slow ripening of QDs, giving more room for manipulations with them. If strained InGaAs islands are covered with a thin GaAs layer, islands in a second sheet are

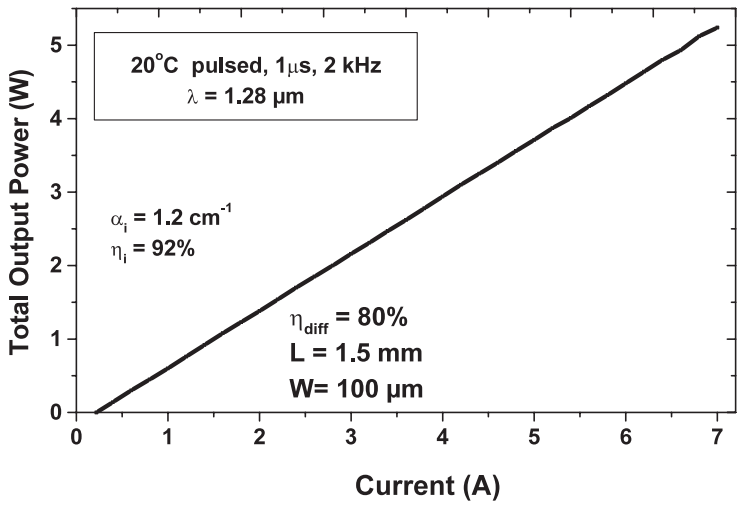

Figure 1. Output power versus injection current for a laser based on self-organized InAs–GaAs QDs. Five-fold stacked QDs are used as an active media. At highest currents the emission wavelength approaches 1.3 μm.

formed over the dots in the first sheet, resulting in a three-dimensional ordered array of QDs, either isolated or strongly vertically coupled [1, 4]. The size and shape of the InGaAs islands can be changed by replacing InAs by InGaAs or InGaAlAs and by changing the deposition mode.

A promising way of achieving long-wavelength emission from GaAs-based QDs is to use activated alloy phase separation. It is based on the controlled increase of the volume of the initially small strained island by alloy overgrowth and was demonstrated for InAs QDs on GaAs substrates covered by a (In,Ga)As layer [26, 27]. Once the dots are covered by InGaAs alloy, it is energetically favourable for InAs molecules to nucleate at the elastically relaxed islands, where the lattice parameter is close to that in the unstrained InAs. An alternative approach is based on seeding small QDs followed by the overgrowth of larger ones [9].

3. Edge-emitting lasers

3.1. Basic characteristics

To date we have indeed demonstrated a record low transparency current of 6 A cm^{-2} per dot layer high power of 4 W CW, an internal quantum efficiency of 98% and an internal loss below 1.5 cm^{-1}, both at 1.16 μm [28] and 1.3 μm (see figure 1) [17]. High-power pump lasers at 1.16 μm wavelength are of most importance for novel colour display systems based on Tm^{3+} doped fluoride fibres, and 1.3 μm lasers are widely used in data communications systems. Output powers of QD lasers operating below 1.3 μm in the range of 4–6 W CW are realized [29].

GaAs-based QD lasers based on three-fold stacked QDs emitting at 1.3 μm with $J_{th} = 70$ A cm^{-2} show a CW output power of $\sim$3 W. The estimated maximum modal gain for the QD ground state lasing is about 14 cm^{-1} and can be increased up to 35 cm^{-1} for ten-fold-stacked QD active regions [13].

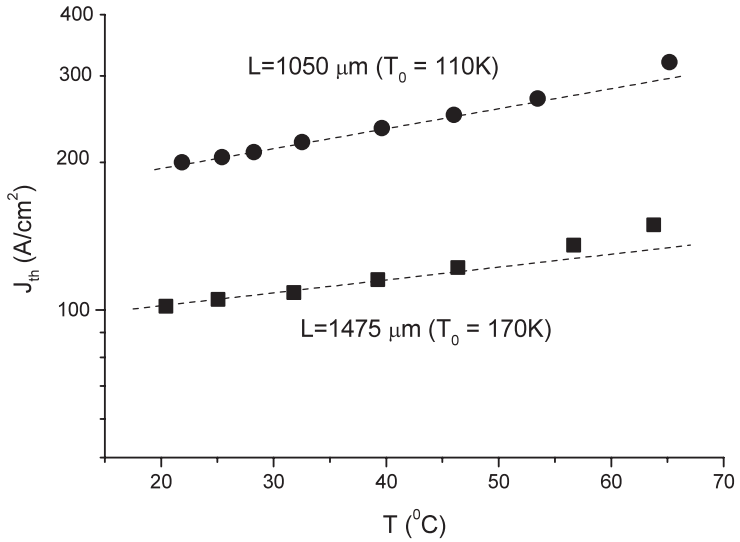

Figure 2. Threshold current density versus temperature for edge-emitting laser based on five-fold stacked QDs. The results are shown for two different cavity lengths. Uncoated facets are used.

3.2. Temperature stability

Already the first injection lasers based on self-organized QDs demonstrated ultrahigh characteristic temperatures (T_0) in a temperature range below 150–180 K [13]. However, at room temperatures, the threshold current was much less temperature-stable. Several approaches to reach high T_0 values were proposed, including placing of QDs into a GaAs–AlGaAs QW [30] or by p-doping of QDs. In spite of the fact that very high T_0 values were obtained (for example, the T_0 close to 230 K up to 330 K is reported in [31]), the penalty is the reduced differential efficiency (<20% in [31]). Recently [16, 17], using defect-free stacked QDs, it became possible to increase the T_0 value to 170 K (up to 60 °C) without paying a penalty of increased internal losses (see figure 2). This enabled 1.3 μm GaAs devices which can operate at 85% differential efficiency, low threshold current density (100 A cm^{-2}, 1.5 mm cavity length, uncoated) and high characteristic temperature, with all the parameters realized in the same device.

3.3. Single-mode operation and filamentation problem

Narrow 7 μm-wide stripes were also fabricated from similar wafers. Low threshold single-transverse-mode kink-free operation up to 330 mW was demonstrated for uncoated facets (see figure 3) [11, 27]. Such a good performance is a direct consequence of the reduced light and current filamentation observed in QD lasers, which is described by the linewidth enhancement factor (α factor). On the one side, carrier localization in QDs strongly reduces spreading of nonequilibrium carriers and their redistribution. On the other side, the filamentation problem arises due to the refractive index modulation dependence on the injection current. The change in the current causes a change in the gain spectrum and, according to the Kramers–Kronig equations, the change in the resonant component of the refractive index of the active media spectrally coincides with the range of the lasing wavelength. Areas with local fluctuation of the current may thus confine the light wave, which in turn causes redistribution of nonequilibrium

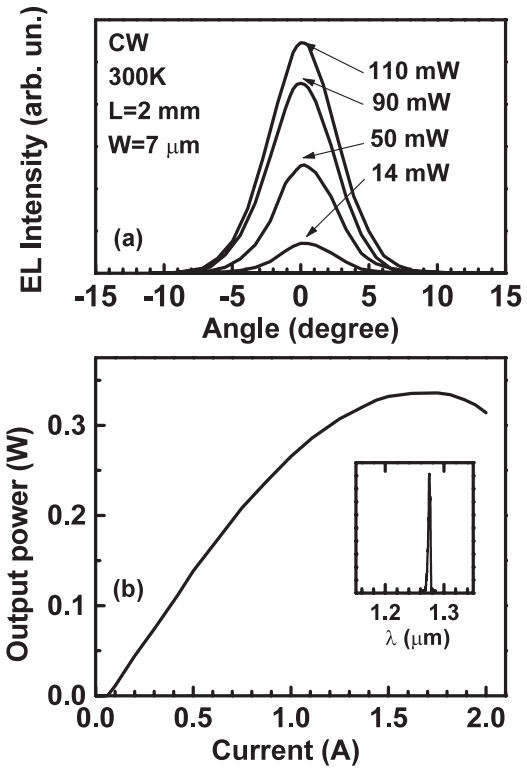

Figure 3. High-power kink-free single-mode operation of long-wavelength QD laser.

carriers and a positive feedback arises. As the ground state gain peak of typical QDs is highly symmetric and the lasing energy is close to the gain maximum [1, 11], the α factor in QD lasers is very small and the filamentation is thus suppressed.

In figure 4(a) we show near-field patterns of the GaAs-based lasers grown in a similar epitaxial design and processed in similar shallow-mesa stripes on: QW emitting at 1.1 μm, QDs emitting at 1.1 μm and QDs emitting at 1.3 μm. It is clearly seen from figure 4(a) that for a similar lasing wavelength of 1.1 μm, a similar epitaxial design and growth equipment (MOCVD) and similar processing the near-field is much more strongly laterally expanded with respect to the geometrical stripe width (6 μm) of the devices in the QW laser. This is a consequence of the more pronounced nonequilibrium carrier spreading, in addition to the current spreading in the QW laser.

Another important feature is clearly revealed near-field filamentation in the QW laser (see figure 4(b)), which is not observed in QD devices for the same output power of 60 mW. The filamentation seen in the QW laser occurs on a length scale of 1 μm. Even the power density per unit facet length is smaller than in the QD lasers due to enhanced carrier spreading in the QW device.

The key parameter, characterizing the beam quality M^2, which characterizes the possibility of focusing the laser beam, or to convert it to a parallel beam, is strongly related to the filamentation problem. In figure 5 we show the dependence of the lateral beam width versus the distance along the propagation axis for the QD and QW lasers. This dependence is used to define the beam quality M^2, as described by Ribbat *et al* [27]. It is clear from the figure that

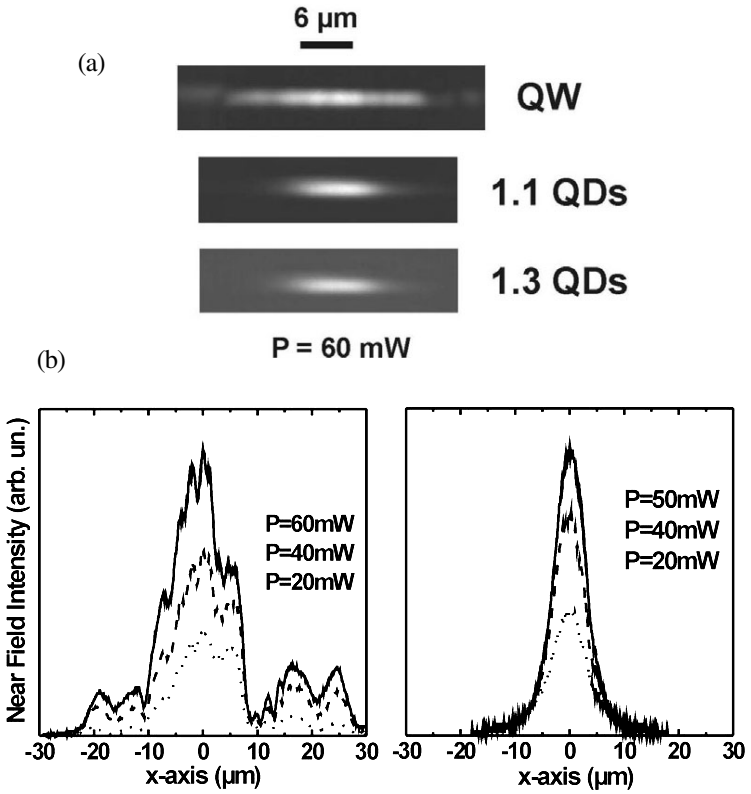

Figure 4. (a) Near-field patterns for the GaAs-based lasers grown in similar epitaxial designs and processed in similar shallow-mesa stripes based on: QW emitting at 1.1 μm (top), QDs emitting at 1.1 μm (middle) and QDs emitting at 1.3 μm (bottom). (b) Near-field intensity recorded along the stripe facet for 1.1 μm QW (left) and 1.3 μm QD (right) lasers for different output powers.

the beam quality is much better for the QD device, as would be expected from the near-field studies. The M^2 values acceptable for the major device applications are below 2.

Figure 6 summarizes the beam quality of the QW and QD lasers emitting at 1.1 and 1.3 μm wavelength as a function of the geometrical stripe width. It follows from the figure that 1.3 μm lasers provide excellent M^2 values up to 9 μm geometrical stripe widths. This is because of the stronger suppression of the nonequilibrium carrier diffusion in deeper QDs and the lower α factor due to the weaker influence of the excited QD and continuum states on the symmetric ground state gain spectrum in long-wavelength QD structures [27].

3.4. Mode grouping

It was found that the lasing spectrum of ridge-stripe QD lasers demonstrates a remarkable tendency towards longitudinal mode grouping, resulting in formation of multiple quasi-equidistant peaks in the lasing spectrum [32]. According to the temperature dependence of the peaks they were attributed to the impact of the Fabry–Perot (FP) resonator formed perpendicular to the ridge on the gain spectrum in the longitudinal direction. Several other effects have been proposed to explain such modulations. Leaky modes, propagating into the substrate, were claimed as the most probable origin of modulations with a quasi-periodicity of

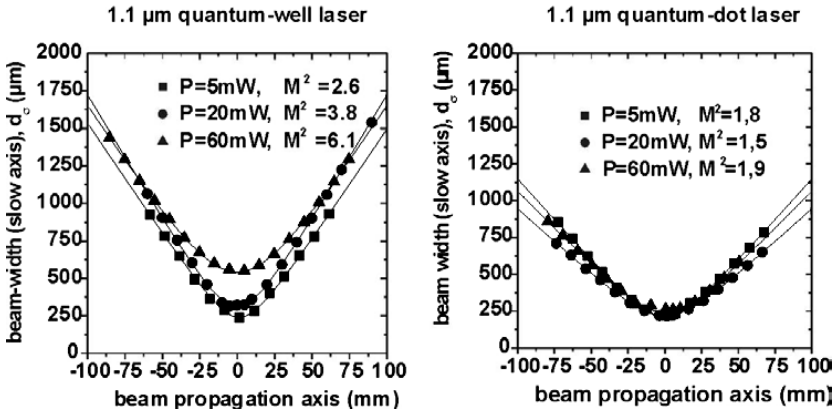

Figure 5. The dependence of the lateral beam width along the propagation axis for the QD and QW lasers.

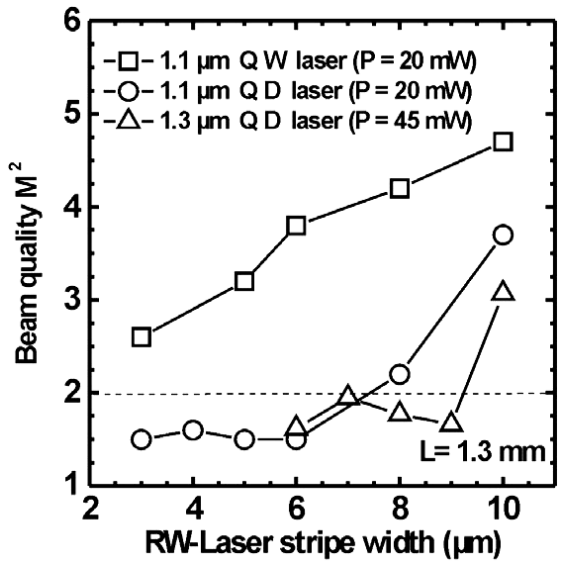

Figure 6. Comparison of the beam quality (M^2) of the QW and QD lasers emitting at 1.1 and 1.3 μm wavelength as a function of the geometrical stripe width.

$\sim$3–5 nm for substrate thicknesses of 100–200 μm [33, 34]. Alternatively, the peak-to-peak energy separation in the intensity-modulated lasing spectra was related to the homogeneous linewidth of QD transitions at room temperature [35]. This research was performed, however, mostly on ridge stripes of only one fixed width, making it difficult to judge the origin of the mode grouping.

In figure 7 we show the dependence of the characteristic distance between the valleys in the lasing spectrum on the ridge stripe width [36]. It is clearly seen that the mode group spacing strongly increases with decreasing stripe width, showing the impact of the hole burning effect in the inhomogeneous spectral gain profile of the QDs on lasing in the longitudinal direction. It was proposed [36] that the effect can be used intentionally to ensure better control over the lasing spectrum of QD lasers.

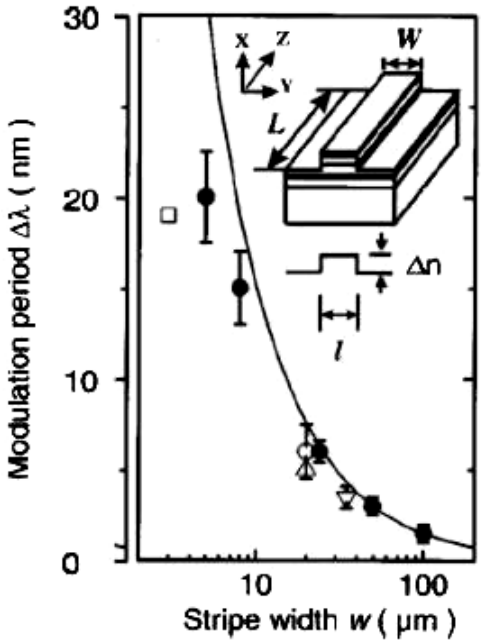

Figure 7. The dependence of the characteristic distance between the valleys in the lasing spectrum on the ridge stripe width. The experimental points are taken according to different authors, as explained in [36].

3.5. Operational lifetime and accelerated degradation tests

QD lasers demonstrate enhanced resistivity in temperature-accelerated degradation tests. Operational lifetimes in excess of 400 h CW at 60 °C at output powers in excess of 300 mW without any noticeable degradation are demonstrated for the devices tested without facet protection in a humid room ambience [37]. In contrast, QW devices demonstrate >10% degradation of the output power already after 100 h CW operation under otherwise similar operational conditions. Facet coated broad-area devices demonstrating quasi-CW operation (4:1 duty cycle) up to 12 W [38] were also tested. They demonstrated operational lifetimes at 1.5 W CW operation at 50 °C exceeding 3000 h [38].

An enhanced stability of QD devices was also revealed in intentional degradation tests using high-energy proton bombardment [18]. The increase in the threshold current after the treatment was twice as small in QD devices as compared to QW lasers, even if the initial characteristics were similar (figure 8).

3.6. Time response

Time response is a key issue for most of the commercial applications in telecommunications. The ground state luminescence evolution times in QDs are in the range of only 10–40 ps, depending on the particular geometry of QDs even at low excitation densities and observation temperatures [39]. At high excitation densities and temperatures the times can be reduced further due to the higher role of multi-particle relaxation processes. These capture times are far shorter than in the bulk, where luminescence rise times as long as 4 ns have been reported at low temperatures in high-purity material [40]. Thus, the phonon bottleneck for carrier relaxation

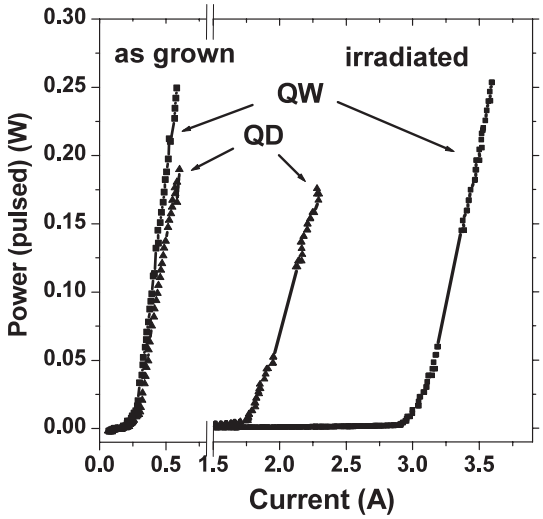

Figure 8. Optical output power versus current in pulsed operation for the QW and QD lasers with similar designs before and after irradiation. (1.6 mm cavity length, 200 μm stripe width.)

is not a major concern for QD lasers and the devices operating at 20–100 Gb s^{-1} can be potentially realized. Relaxation oscillations indicate the potential for modulation bandwidths larger than 6 GHz (see figure 9, [41]). Thus, high-speed TDM systems based on QD lasers are now possible. The practical limitation of high-frequency operation at high temperatures can be, most probably, the cavity reservoir effect due to carrier accumulation in the regions surrounding QDs at elevated temperatures, as is also the case for QW devices.

Recently, it was shown that the concept of resonant carrier injection into QDs [42] enables realization of devices operating at 15 GHz at room temperature [43]. Modulation doping of QDs with acceptors is expected to increase the high-frequency response of QD lasers beyond 20 GHz [44]. Oxide-confined two-section bistable QD 1.3 μm lasers with an integrated intracavity saturable absorber demonstrated passive mode locking at a repetition rate of 7.4 GHz with a duration of 17 ps [45]. These results suggest that a carefully designed QD laser is also a candidate for ultrashort pulse generation [46].

4. Vertical cavity surface-emitting lasers

There is a need for cost-effective vertical cavity surface-emitting lasers (VCSELs) emitting at 1.3 μm. The currently existing FP and distributed feedback (DFB) devices grown on InP substrates are rather expensive. In contrast, GaAs-based VCSELs are proven to have high reliability, very low cost and superb parameters, such as low beam divergence, high wall-plug efficiency and high temperature stability of the emission wavelength and threshold current. The possibility of on-chip testing and integration, a significant reduction of lateral size, lateral arrays and beam steering are advantageous. At the same time GaAs-based VCSELs emitting at 850–940 nm, are extremely cost-efficient, but operate only at distances below 300 m. The setbacks of the existing InP- and GaAs-based devices will help 1.3 μm GaAs VCSELs to replace both InP-based FP and DFB lasers and also 0.85 μm GaAs VCSELs.

An additional advantage of VCSELs is the possibility of vertical integration of a device with wavelength modulators (e.g. for chirp compensation), intensity modulators and photodetectors, which is very important for advanced applications in wavelength division

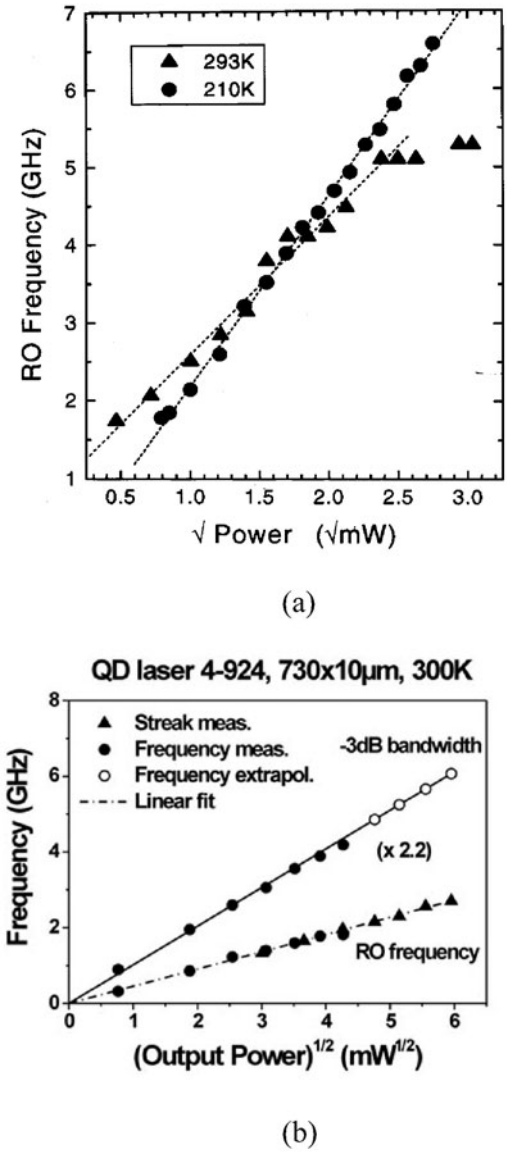

Figure 9. (a) Relaxation oscillation frequency of a 1.1 μm QD laser as a function of power. $f_{3\,\mathrm{dB}} = 10.2$ and 8.2 GHz for 210 and 293 K, respectively. (b) Time response of a 1.3 μm QD laser as a function of power. $f_{3\,\mathrm{dB}}$ is up to 6 GHz for 300 K at high operating currents. QD laser no. 4-924 contains ten-fold stacked QDs in the active region.

multiplexing (WDM). VCSELs have an important counterpart—cavity enhanced selective photodetectors allowing dense WDM (DWDM), data transmission links and ultrafast data traffic using electronically wavelength tunable VCSELs. Both electronic (electrooptic) and membrane tuning of the wavelength can be used for DWDM and, of course, WDM (CWDM). The development of optical fibres, which do not contain the water absorption hump between 1.3 and 1.55 μm range, further extends the DWDM range and potentially merges DWDM and CWDM applications.

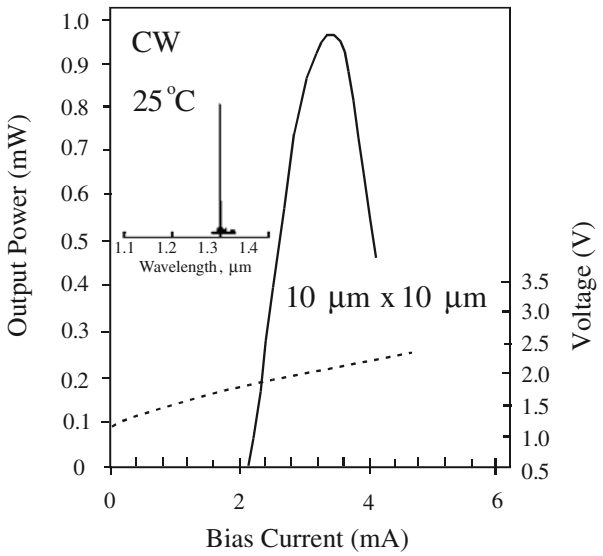

Figure 10. CW L–I–V curves of the 1.3 μm-emitting GaAs-based QD VCSEL. The device has an oxide-confined aperture with lateral dimensions 10 μm × 10 μm.

The major problem for cost-efficient long-wavelength InP-based VCSELs and relevant vertical cavity devices is the lack of adequate native DBRs. Mirrors based on layers lattice-matched to InP have small refractive index differences and very low heat conductivity. An InGaAsP/InP Bragg mirror with 50 or more periods is required to achieve the reflectivity ($R = 0.99$) required for lasing. The bonding of GaAs/AlGaAs Bragg mirrors to InP-based active regions may solve the problem, but it represents a very complex technology and is expensive for large-scale production. Other recent approaches (using top metamorphic AlAs–GaAs DBR, or using AlGaAsSb-based DBRs on InP substrates) do not solve the problem of reliability and cost efficiency, and may be competitive only until the production-oriented GaAs-based technology is developed.

We presented the first GaAs VCSEL for operation at 1.3 μm [13, 47, 48]. The microcavity was surrounded by (p) and (n) $Al_{0.98}Ga_{0.02}As$ layers ($<\lambda/4$ thick) followed by 1λ-thick (p) and (n) GaAs current spreading/intracavity contact spacer layers doped to 10^{18} cm^{-3}. Intracavity contacts were used. The spacer layers were followed by DBRs composed of alternating $Al_{0.98}Ga_{0.02}As$ and $\lambda/4$-thick GaAs layers. The $Al_{0.98}Ga_{0.02}As$ layers in the DBR, as well as those surrounding the optical cavity, were selectively oxidized to form Al(Ga)O. The QDs are centred in a 1λ-thick GaAs optical microcavity, whose edges are doped to 10^{17} cm^{-3}. The ends of the microcavity are composed of $Al_xGa_{1-x}As$ linearly graded from $x = 0.02$ up to 0.98. The CW light power–current–voltage (L–I–V) characteristics of a QD VCSEL are shown in figure 10.

It was shown that the threshold current of the QD VCSEL remains practically unchanged with temperature increase [49]. The electroluminescence measurements from QD LED test structures indicate that the lasing proceeds via the QD ground state transition. The maximum differential efficiency is above 90%. The emission wavelength was near 1.3 μm (1.28–1.306 μm), depending on the particular position on the wafer. Variation in the threshold current across the wafer was ∼10%. We found that the threshold current demonstrates only weak dependence on the aperture size down to submicrometre cavities, while the photon confinement effect leading to a blue shift of the lasing emission becomes

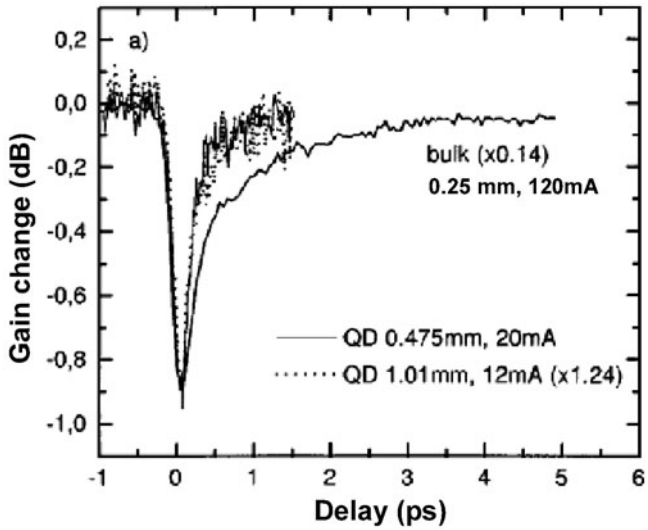

Figure 11. Comparison between the phase changes in the QD and in the bulk device. The gain change for the bulk double heterostructure laser is shown by the full curve.

increasingly important. During the lifetime test in excess of 5000 h CW at 60 °C no change in the performance of the devices was found.

5. QD amplifiers

Amplifiers based on QDs show, at room temperature, phase relaxation times of <50 fs and gain recovery times as short as 140 fs, much faster than QW-based ones (figure 11), indicating the potential of QDs for a completely novel class of devices with large commercial importance in particular for metropolitan area networks [16, 17, 25].

In figure 11 we show the comparison of gain dynamics measured on a bulk InP-based device at the maximum achievable small signal gain (13 dB) with the gain dynamics of the QD device at 20 mA. The bulk device shows a clear carrier heating recovery on a 1 ps scale [21, 50]. The QD device dynamics is 4–7 times faster [50]. Comparison at different bias currents showed that heating due to free-carrier absorption is reduced in QD devices compared to the bulk case.

6. Conclusion

QD devices emerged from their early stage and quickly moved towards the most commercially relevant applications in optoelectronics. Further work will concentrate on the expansion of GaAs-based QD lasers towards the 14XX nm spectral range necessary for Raman amplifiers and towards the 15XX–16XX nm spectral range important for transmitters, particularly for GaAs-based wavelength-tunable VCSELs. Work in this direction has already started.

Acknowledgments

This work is carried out in cooperation with V M Ustinov, A R Kovsh, A E Zhukov, R Sellin, C Ribbat, M Laemmlin, J A Lott, P Borri and J Hvam. It is supported in different parts by NanOp CC, Deutsche Forschungsgemeinschaft (Sfb296), Dotcom, Volkswagen Foundation, INTAS, and the Russian Foundation for Basic Research. NNL acknowledges a Mercator Professorship.

References

[1] For a review see
Bimberg D, Grundmann M and Ledentsov N N 1999 *Quantum Dot Heterostructures* (Chichester: Wiley)
[2] Shchukin V A, Ledentsov N N and Bimberg D 2003 *Epitaxy of Nanostructures* (Berlin: Springer)
[3] Bimberg D *et al* 1995 *Thin Solid Films* **267** 32
[4] Ledentsov N N *et al* 1996 *Solid-State Electron.* **40** 785
[5] Shchukin V A and Bimberg D 1999 *Rev. Mod. Phys.* **71** 1125
[6] Bimberg D, Heinrichsdorff F, Ledentsov N N and Shchukin V A 2000 *Appl. Surf. Sci.* **159** 1
[7] Bimberg D 1999 *Semiconductors* **33** 1044
[8] Dingle R and Henry C H 1976 Quantum effects in heterostructure lasers *US Patent Specification* 3982207
[9] Arakawa Y and Sakaki H 1982 *Appl. Phys. Lett.* **40** 939
[10] Asada M, Miyamoto M and Suematsu Y 1986 *IEEE J Quantum Electron.* **22** 1915
[11] Bimberg D *et al* 1997 *IEEE J. Sel. Top. Quantum Electron.* **3** 196
[12] Bimberg D *et al* 2000 *Thin Solid Films* **367** 235
[13] Ledentsov N N *et al* 2000 *IEEE J. Sel. Top. Quantum Electron.* **6** 439
Ledentsov N N 2002 *IEEE J. Sel. Top. Quantum Electron.* **8** 1015
[14] Grundmann M and Bimberg D 1997 *Japan. J. Appl. Phys.* **36** 4181
[15] Stier O, Grundmann M and Bimberg D 1999 *Phys. Rev.* B **59** 5688
[16] Ledentsov N N 2002 *IEEE J. Sel. Top. Quantum Electron.* **8** 1015
[17] Ledentsov N N *et al* 1994 *Semiconductors* **28** 832
Kirstaedter N *et al* 1994 *Electron. Lett.* **30** 1416
[18] Ribbat C *et al* 2001 *Electron. Lett.* **37** 174
[19] Tomm J, Sellin R, Ribbat C and Bimberg D unpublished
[20] Borri P *et al* 2000 *IEEE Photonics Technol. Lett.* **12** 594
[21] Borri P *et al* 2000 *IEEE J. Sel. Top. Quantum Electron.* **6** 544
[22] Mirin R 1999 *Adv. Semicon. Lasers Appl.* **153** 21
[23] Sugawara M *et al* 2001 *Japan. J. Appl. Phys.* **40** L488
[24] Shchukin V A, Ledentsov N N, Kop'ev P S and Bimberg D 1995 *Phys. Rev. Lett.* **75** 2968
[25] Ledentsov N N *et al* 2001 *Semicond. Sci. Technol.* **16** 502
[26] Shernyakov Yu M *et al* 1999 *Electron. Lett.* **35** 898
[27] Maximov M V *et al* 2001 *IEEE J. Quantum Electron.* **37** 676
Ribbat Ch *et al* 2003 *Appl. Phys. Lett.* **82** 952
[28] Sellin R, Ribbat Ch, Grundmann M, Ledentsov N N and Bimberg D 2001 *Appl. Phys. Lett.* **78** 1207
[29] Mikhrin S S *et al* 2002 *Proc. 26th Int. Conf. on the Physics of Semicond.* at press
[30] Maximov M V *et al* 1997 *Japan. J. Appl. Phys.* 1 **36** 4221
[31] Shchekin O B *et al* 2002 *Electron. Lett.* **38** 712
[32] Zaitsev S V *et al* 1997 *Semiconductors* **31** 455
[33] O'Reilly E P *et al* 1998 *Electron. Lett.* **34** 2035
[34] Patanè A *et al* 2000 *J. Appl. Phys.* **87** 1943
[35] Sugawara M, Mukai K, Nakata Y, Ishikawa H and Sakamoto A 2000 *Phys. Rev.* B **61** 7595
[36] Ouyang D *et al* 2002 *Appl. Phys. Lett.* **81** 1546
[37] Lundina E Yu *et al* 2003 *Tech. Phys.* **48** 131
[38] Sellin R L *et al* 2002 *Electron. Lett.* **38** 883
[39] Ledentsov N N *et al* 1996 *Phys. Rev.* B **54** 8743
[40] Aaviksoo J *et al* 1992 *Phys. Rev.* B **45** 1473
[41] Bimberg D *et al* 2001 *Phys. Status Solidi* b **224** 787
[42] Asryan L V and Luryi S 2001 *IEEE J. Quantum Electron.* **37** 905
[43] Bhattacharya P and Ghosh S 2002 *Appl. Phys. Lett* **80** 3482
[44] Shchekin O B and Deppe D G 2002 *Appl. Phys. Lett.* **80** 2758
[45] Huang X *et al* 2001 *Appl. Phys. Lett.* **78** 2825
[46] Wonfor A *et al* 2002 *Lasers and Electro-Optics Society LEOS 2002. The 15th Annu. Mtg of the IEEE* vol 1 (New York: IEEE) p 21
[47] Ledentsov N N *et al* 2000 *Memoirs of The Institute of Scientific and Industrial Research (Osaka)* vol 57 p 80
[48] Lott J A *et al* 2000 *Electron. Lett.* **36** 1384
[49] Ledentsov N N *et al* 2002 *Japan. J. Appl. Phys.* 1 **41** 949
[50] Borri P *et al* 2001 *Phys. Status Solidi* b **224** 419